BILINGUAL PUBLISHING GROUP

Journal of Architectural Environment & Structural Engineering Research

https://journals.bilpubgroup.com/index.php/jaeser

ARTICLE

Fatigue Safety Assessment of Concrete Continuous Rigid Frame Bridge Based on Rain Flow Counting Method and Health Monitoring Data

***Yinghua Li*[1], *Junyong He*[2*], *Xiaoqing Zeng*[3], *Yanxing Tang*[4]**

[1] *Shixing County Administrative Service Center, Shixing, Shaoguan, Guangdong, 512500, China*

[2] *Guangdong College of Industry and Commerce, Guangzhou, Guangdong, 510510, China*

[3] *Shixing County Statistics Bureau, Shixing, Shaoguan, Guangdong, 512500, China*

[4] *Shixing County Hospital of Traditional Chinese Medicine, Shixing, Shaoguan, Guangdong, 512500, China*

ABSTRACT

The fatigue of concrete structures will gradually appear after being subjected to alternating loads for a long time, and the accidents caused by fatigue failure of bridge structures also appear from time to time. Aiming at the problem of degradation of long-span continuous rigid frame bridges due to fatigue and environmental effects, this paper suggests a method to analyze the fatigue degradation mechanism of this type of bridge, which combines long-term in-site monitoring data collected by the health monitoring system (HMS) and fatigue theory. In the paper, the authors mainly carry out the research work in the following aspects: First of all, a long-span continuous rigid frame bridge installed with HMS is used as an example, and a large amount of health monitoring data have been acquired, which can provide efficient information for fatigue in terms of equivalent stress range and cumulative number of stress cycles; next, for calculating the cumulative fatigue damage of the bridge structure, fatigue stress spectrum got by rain flow counting method, S-N curves and damage criteria are used for fatigue damage analysis. Moreover, it was considered a linear accumulation damage through the Palmgren-Miner rule for the counting of stress cycles. The health monitoring data are adopted to obtain fatigue stress data and the rain flow counting method is used to count the amplitude varying fatigue stress. The proposed fatigue reliability approach in the paper can estimate the fatigue damage degree and its evolution law of bridge structures well, and also can help bridge engineers do the assessment of future service duration.

Keywords: Long-span continuous rigid frame bridge; Rain flow counting method; Fatigue performance; Health monitoring system; Strain monitoring data

*CORRESPONDING AUTHOR:

Junyong He, Guangdong College of Industry and Commerce, Guangzhou, Guangdong, 510510, China; Email: 418474986@qq.com

ARTICLE INFO

Received: 10 August 2023 | Revised: 30 August 2023 | Accepted: 15 September 2023 | Published Online: 12 October 2023

DOI: https://doi.org/10.30564/jaeser.v6i3.5890

CITATION

Li, Y.H., He, J.Y., Zeng, X.Q., et al., 2023. Fatigue Safety Assessment of Concrete Continuous Rigid Frame Bridge Based on Rain Flow Counting Method and Health Monitoring Data. Journal of Architectural Environment & Structural Engineering Research. 6(3): 31-40. DOI: https://doi.org/10.30564/jaeser.v6i3.5890

1. Introduction

Due to the influence of materials ageing, environmental corrosion, increasing traffic flow and other factors, at present, a large number of concrete structures in China and other countries in the world are gradually ageing, and the deterioration of structures is becoming more and more serious [1,2], resulting in damage accumulation and resistance attenuation. Therefore, the fatigue properties of concrete structures and their components have been paid more and more attention by people around the world.

The fatigue reliability assessment of reinforced concrete structures has been studied by many experts and scholars, and many research results have been published [3-9]. Generally, the fatigue failure of concrete structures is mainly caused by the stress cycle. In most cases, the stress cycle of the concrete structure is a variable amplitude stress cycle, for example, temperature, vehicle live load, etc., rather than the constant amplitude stress cycle used in the test, and the combination of variable amplitude stress is too much, and so it is difficult to simulate in the test. Hence, there are few research results on the fatigue performance of concrete bridges based on in-situ measured data. John P. Li Z X, Chan T H T et al. [10,11] paid attention to developing a methodology for fatigue damage assessment and life prediction of bridge-deck sections of existing bridges with monitoring data of online HMS, and applied the method to the Tsing Ma Bridge for the fatigue damage assessment. By using the Palmgren-Miner rule and S-N curves, Guo, Tong, Li, et al. [12] made an assessment for welded joints in orthotropic steel decks based on monitored field data from the Runyang Bridge. Kwon K and Frangopol D M [13] focus on fatigue reliability assessment of steel bridges by using probability density functions of equivalent stress range based on field monitoring data and they suggested the method should be applied to two bridges. Yang D, Youliang D, Aiqun LI, et al. [14] suggest a reliability assessing methodology of fatigue life for welded details in steel box girder based on the long-term monitoring data, and the application research is presented with examples of welded rib-to-deck details in Runyang Bridges. Newhook and Rahman Edalatmanesh [15] explained that the concepts of reliability and HMS can be integrated to do bridge assessments and make decision systems. Junges P et al. [16] assess the fatigue life of the bridges with only 120 days of monitoring data and using S-N curves from international standards. Mankar A. et al. [17] suggested a probabilistic reliability framework for the assessment of future service duration for civil infrastructure, including probabilistic modelling of actions with a large amount of monitoring data, and also containing probabilistic modelling of fatigue resistance by test data, and a case study is presented for the steel-reinforced concrete slab.

In brief, the in-situ monitoring data of prestressed concrete bridge structures are either with short monitoring time or no monitoring data. Hence, in the paper, applying a large amount of strain monitoring data, based on structural fatigue damage accumulation theory, a method is presented to study the evolution of fatigue properties and the cumulative changing law of fatigue damage of a prototype bridge, which is Long-span continuous rigid frame bridge with HMS.

2. Basic theory of fatigue effects

2.1 Miner theory

The cumulative damage theory of fatigue is needed to estimate the effects of varying amplitude stress cycles on structures. The theory of linear fatigue cumulative damage means that under cyclic load, fatigue damage can be linearly accumulated, and each stress is independent and unrelated to the other. When the cumulative damage reaches a certain value, fatigue damage of specimens or components will occur. A typical linear cumulative damage theory is Palmgren-Miner theory, referred to as the Miner theory [18]. Under variable amplitude load, the damage formula caused by n cycles can be written as follows:

$$D = \sum \frac{n_i}{N_i} \tag{1}$$

The theory states that if the material is subjected to a load of magnitude $\sigma_{\alpha i}$ with repeating N_i times of failure, the damage can be distributed linearly to each cycle; that is, the damage to the material per cycle is $\frac{1}{N_i}$. If the load of magnitude $\sigma_{\alpha i}$ rings n_i, the damage of the material is $\frac{n_i}{N_i}$. Under different load effects, the damage is $\frac{1}{N_1}, \frac{1}{N_2}, \ldots$ respectively. When the total damage reaches 1, the structure fatigue failure occurs. That is, the criterion of material fatigue failure is:

$$D = \sum \frac{n_i}{N_i} = \frac{1}{N_1} + \frac{1}{N_2} + \cdots + \frac{n}{N_n} = 1 \tag{2}$$

where, D is the damage degree of the structure; n_i is the number of stress cycles that the structure actually experiences with the magnitude $\Delta\sigma_i$; N_i is the fatigue life of the structure under the action of $\Delta\sigma_i$.

2.2 Fatigue damage theory of concrete materials used in the prototype bridge

In order to conduct fatigue reliability analysis of bridge members or structural details, it is necessary to understand the time history of stress amplitude in the member or structure, and conduct statistical analysis of load effects $\Delta\sigma_e$; that is, the variation situation of amplitude variation repeated stress in the details under the action of actual loads. By monitoring the stress history of the main components or details, the stress time history curve of the components or details under the action of actual load effects can be obtained.

In addition to the fatigue stress spectrum, S-N curves and damage criteria are also needed for fatigue damage analysis. An overview of experimental research on the fatigue working characteristics of concrete under multi axial complex stress states has been conducted by Song Yupu et al. from the Dalian University of Technology [19], which comprehensively and deeply describes the changes in mechanical properties of concrete under multi-axial fatigue states, and the S-N curve method for calculating the fatigue strength of concrete under various working states has been established. The research results can be applied to the fatigue design of concrete bridges, crane beams, offshore platforms, concrete sleepers, nuclear safety shells, pressure vessels, and other structures, and provide references for the formulation of relevant specifications. So, in this paper, the research results of Song Yupu et al. are adopted. The ratio of minimum stress to maximum stress is taken as the third variable in the S-N curve. The S-N relationship of concrete under pressure can be expressed as follows:

$$\sigma_{\max} / f_{cm} = 1 - \beta(1 - R)\lg N \tag{3}$$

In the formula, f_{cm} is uniaxial compressive strength of concrete; $R = \sigma_{\min} / \sigma_{\max}$ is the minimum stress to maximum stress ratio in the stress cycle; $\beta = 0.072$ is the material constant. The fatigue damage criterion adopts Miner linear cumulative damage criterion, as shown in Equations (1) and (2).

Assuming that the maximum and minimum stresses of the mid-span web and bottom plates of the bridge acquired by the monitoring system are $\Delta\sigma_{i\max}$ and $\Delta\sigma_{i\min}$ respectively, according to Miner theory and Equation (3), we can get:

$$N_{\Delta\sigma_i} = 10^{\frac{1-\frac{\Delta\sigma_{i\max}}{f_{cm}}}{\beta(1-R_{\Delta\sigma_i})}} \tag{4}$$

where, $N_{\Delta\sigma_i}$ is the number of fatigue failure cycles under the amplitude varying stress $\Delta\sigma_i$, $R_{\Delta\sigma_i} = \Delta\sigma_{i\min} / \Delta\sigma_{i\max}$. Then, the fatigue damage of the positions embedded with sensors caused by one load of the amplitude varying stress $\Delta\sigma_i$ is as follows:

$$D_{\Delta\sigma_i} = \frac{1}{N_{\Delta\sigma_i}} = 10^{-\left(\frac{1-\frac{\Delta\sigma_{i\max}}{f_{cm}}}{\beta(1-R_{\Delta\sigma_i})}\right)} \tag{5}$$

Combining the Miner's rule of linear damage accumulation and Equation (5), an evaluation formula is formulated as follows:

$$L(T_s) = 1 - \sum_{i=1}^{m}\sum_{j=1}^{n} 10^{-\left(\frac{1-\frac{\Delta\sigma_{ij\max}}{f_{cm}}}{\beta(1-R_{\Delta\sigma_{ij}})}\right)} \tag{6}$$

In the formula, T_s is the service duration of the bridge structure; m is the observed number of the different amplitude varying stress $\Delta\sigma_{ij}$; n is the ob-

served number of the specific amplitude stress $\Delta\sigma_{ij}$.

3. Background bridge introduction with HMS

3.1 The health monitoring system installed on the bridge

The sample bridge adopted in the paper is located in Guangdong Province. The structure of the main beam of the bridge is a (51.4 + 94 + 4 × 144 + 87) m, shown in **Figure 1a** pre-stressed concrete continuous box-beam system, with 8 main piers and 7 main spans. The box girder is a single box and single room section, and the full width of the box girder is 12.5 m, and the width of the bottom plate is 6.8 m. The transverse slope of the bridge floor is 2.0%, and the longitudinal slope of the bridge floor is 0.15%. The whole bridge has 6 closing sections, and the main beam cross section heights change from 8 m to 2.8 m in accordance with the 1.6 order power parabola from the cantilever root to the mid-span. The base plate thickness varies from 1 m to 0.32 m, and the web plate thickness varies from 0.9 m to 0.45 m. The prestressed tendons are $15\Phi^j 15.24\,\text{mm}$ steel strands with strength: $R_y^b = 1860\,\text{MPa}$, $2\Phi^j 12.7\,\text{mm}$ steel strands with strength: $R_y^b = 1395\,\text{MPa}$ and high strength rebar respectively.

The measuring points of the bridge HMS in the main beam are arranged at the root of the cantilever, L/2 span, L/4 span and other key positions, and the bridge has 8 cantilever end sections, 8 L/4 sections and 4 L/2 sections respectively, as shown in **Figure 1b**. **Figure 1c** is the actual photo of the concrete bridge, and the embedded positions of sensors on each section are shown in **Figure 2**. The string type strain gauge (JMZX-215) used in the bridge HMS is shown in **Figure 3**, which can measure the temperature simultaneously and so it is able to compensate for temperature effects. The measuring time interval of the sensor is 1 hour. The parameters of the sensor are shown in **Table 1** and the basic parameters of high performance concrete applied in the bridge are displayed in **Table 2** [20,21]. Among them, the tensile

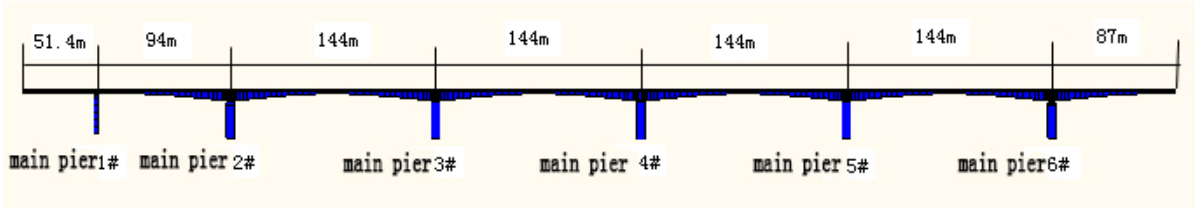

(a) the length of each span of the bridge

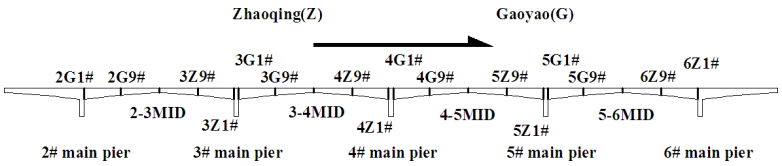

(b) Sketch of the cross section locations with the embedded sensors

(c) The actual photo of the concrete bridge

Figure 1. Sketch of the cross section locations with the embedded sensors and the the length of each span.

Table 1. Parameters of the strain gauge.

Name	Range	Sensitivity	Gauge length	Remarks
Intelligent digital vibrating strain gauge	± 1500 $\mu\varepsilon$	1 $\mu\varepsilon$	157 mm	Strain gauge embedded in concrete

Table 2. The basic parameters of high performance concrete used in the bridge.

Parameters	Young's modulus (units: MPa)	Tensile strength (units: MPa)	Compressive strength (units: MPa)
Mean value	3.45×10^4	3.278	55.12
Standard deviation		0.361	6.063

and compressive strength parameters of the concrete used in the bridge are obtained from actual measurements. The HMS installed in the bridge is still operating normally.

The monitoring data of this bridge has the characteristics of large data volume and multiple types of data. In order to effectively store data, meet multi-user and multi-task requests, and achieve remote real-time display, query, download, and other functions of data, The research group has designed a centralized data management system. The system is composed of three parts: data storage, remote display, and early warning.

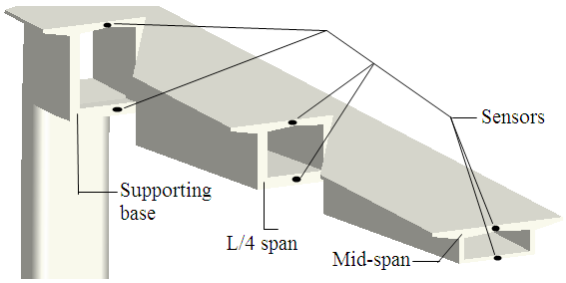

Figure 2. The embedded sensors are locations in the bridge half-span.

Figure 3. Picture of the JMZX-215 sensor.

3.2 The monitoring data processing

In the paper, the data acquired from the sensors named 2-3MID-1, 2-3MID-2, 5-6MID-2, 4Z9h-1 and 4G1h-1 are taken as samples to display the profile of the monitoring data, and the selected time period is from March 2006 to April 2010. The pre-processed method of transforming the initial data into strain data is elaborated in detail in the papers [22,23]. **Figure 4** shows the outline of the strain data after several pre-processed steps. The data interval in the figure below is mainly due to the loss of monitoring data caused by system failure.

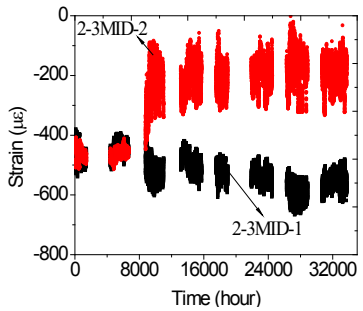

Figure 4. The profile of strain data transformed from the monitored data.

It is assumed that concrete material in the early stage of bridge operation is in the stage of linear elastic change. Combining the Young's modulus value in **Table 2** and the transformed strain data, we can get the stress data. In this paper, the data collected by sensor number 2-3 mid-1 located in the mid-span top plate between the main pier 2# and the main pier 3#, and sensor number 3-4 mid-2 located in the bottom plate between the main pier 3# and the main pier 4# are selected as samples, because the measured data converted to stress data of the mid-span sensors is similar to the principal stress. The selected data of the sensors are located in the middle of the span, and so the converted stress date is basically similar to the principal stress at this position. **Figures 5 and 6**

show the outline of the stress data after pre-processing. As the sensor is embedded in the concrete, the measured data is a comprehensive reflection of the influence factors such as temperature, vehicle load, shrinkage and creep etc. Since the traffic of the background bridge was opened in June 2006, we adopted the data from 2009 for fatigue safety analysis, because the traffic flow, shrinkage and creep and other factors tended to be stable at this time. In order to facilitate data processing by using the rain flow counting methodology, the stress time-history diagram obtained takes stress as the horizontal coordinate and time as the vertical coordinate, as shown in **Figures 4 and 5**. The sample size is 5067 in **Figure 4** and the sample size is 2660 in **Figure 5**, and it is sufficient for statistical analysis.

The compressive stress safety reserve values are converted by the data collected by the sensors during the time after the background bridge is completed and before traffic release. The traffic opening time of the background bridge is in September 2006, and so the stress data acquired at this time is used as the compressive stress safety reserve in accordance with the positions of the sensors 3-4 mid-2 and 2-3 mid-1, and the specific data are shown in **Table 3**. After deducting the compressive stress safety reserve, the stress data can be used for statistics.

Table 3. The compressive stress safety reserve values are in accordance with the positions of the sensors 3-4 mid-2 and 2-3 mid-1.

Sensor number	3-4 mid-2	2-3 mid-1
Compressive stress safety reserve (units: MPa)	–15.1589	–15.8639

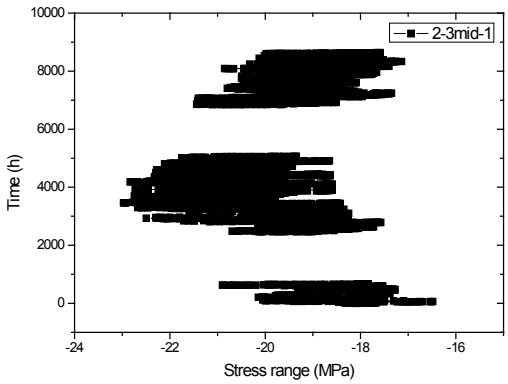

Figure 5. The profile of stress-time curve collected from the sensor 2-3 mid-1 in the whole year 2009.

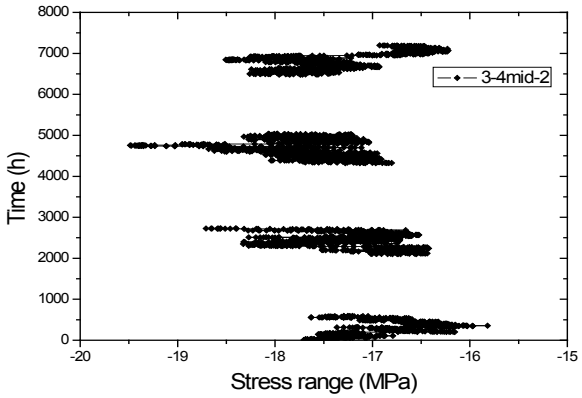

Figure 6. The profile of stress-time curve collected from the sensor 3-4 mid-2 in the whole year 2009.

4. Results and discussion

4.1 Introduction to rain flow counting method

Two British engineers M. Matsuishi and T. Enodo first presented [24] the rain flow counting method in the 1950s. The rain flow counting method's main function is simplifying the measured load history into several load cycles for estimating the fatigue life and compiling the fatigue test load spectrum. According to the two-parameter methodology, dynamic strength (amplitude) and static strength (mean value) are considered, which is in line with the inherent characteristics of fatigue load itself. The methodology is widely used in engineering, particularly in fatigue life calculation. The basic counting rules are as follows:

(1) The rain flow successively flows down the slope from the inner side of the peak position of the load time history;

(2) Rain flow starts from a peak point and stops flowing when it encounters a peak greater than its initial peak;

(3) When the rain stream meets the rain stream flowing down above, it must stop flowing;

(4) Take out all the full cycles and record the amplitude of each cycle;

(5) Equivalent the remaining divergent convergence load time history after the first stage to a convergent and divergent load time history, and then the rain flow count in the second stage is carried out.

The total number of counting cycles is the sum of the counting cycles of the two counting phases.

The main point of the rain flow method is that each part of the load-time history is counted and counted only once, and the damage caused by a large amplitude is not affected by the small loops that truncate it, and the truncated small loops are superimposed on the larger loops and half loops. Therefore, according to the cumulative damage theory, the S-N curve obtained from the constant amplitude experiment and the processing results of the rain flow method can be input into the electronic computer to estimate the fatigue life of the component. Finally, the rain flow counting method is realized by programming with Matlab software [25].

4.2 Statistical results and analysis of stress data with rain flow counting method

For the stress time history data in **Figures 5 and 6**, we treated them with rain flow counting method, and then we got the amplitude varying stress $\Delta\sigma_{ij}$ and the mean with a quantity of 422 each of the data of **Figure 5**, the amplitude varying stress $\Delta\sigma_{ij}$ and the mean with a quantity of 362 each of the data of **Figure 6**. Then, we perform a histogram statistical analysis on the obtained data of the amplitude varying stress $\Delta\sigma_{ij}$ and the mean, the specific statistical results are shown in **Figures 7 and 8**:

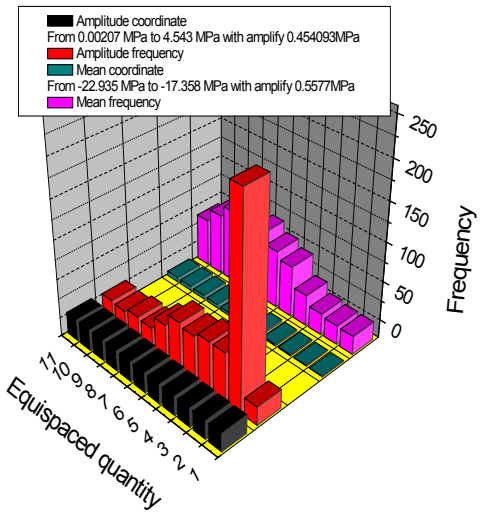

Figure 7. The histogram of the data dealt with in the whole year 2009 of the sensor 2-3 mid-1.

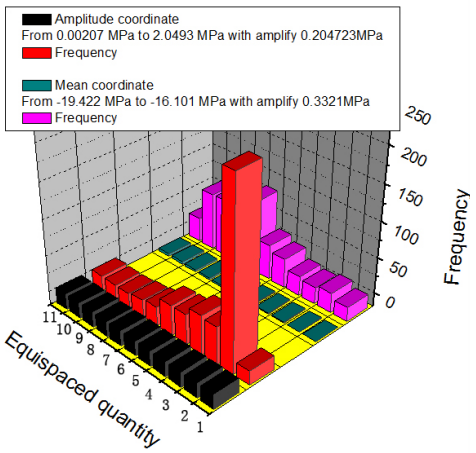

Figure 8. The histogram of the data dealt with in the whole year 2009 of the sensor 3-4 mid-2.

As seen from **Figures 7 and 8**, the range of stress amplitude $\Delta\sigma_{ij}$ false variation is 0.0027 ~ 4.543 MPa and the range of mean variation is –7.0711 ~ –1.4941 MPa in **Figure 7**; the range of stress amplitude $\Delta\sigma_{ij}$ false variation is 0.0027 ~ 2.0493 MPa and the range of mean variation is –4.2631 ~ –0.9421 MPa of **Figure 8**.

4.3 Fatigue damage calculation and evolution law of the prototype bridge

Due to the sensor used in the background bridge equipped with the function of collecting temperature data simultaneously, Li et al. [26] have carried out statistical analysis by using 1 year's temperature monitoring data, and it is found that there are two wave peaks, as shown in **Figure 9**. In the meanwhile, the range of seasonal temperature variation of the bridge is obtained by statistics of the monitoring temperature data, and the temperature stress envelope of the top plate and bottom plate of the bridge is calculated by simulation software, seen in **Figure 10**. It can be seen from the temperature stress envelope diagram that the maximum temperature combined stress variation of the top and bottom in the mid-span is about 6 MPa. Therefore, we believe that the temperature induced stress changes account for a major part of the internal force of the bridge structure. Due to the slow change period of temperature and other changes, the computation times of fatigue damage calculation in this paper are calculated by half a year.

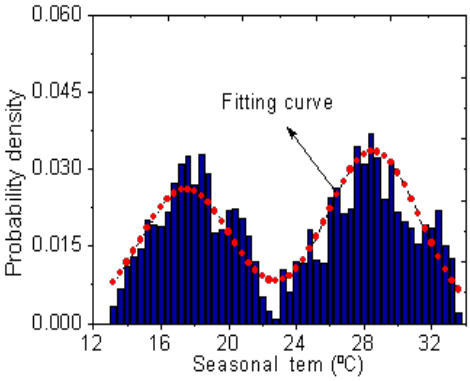

Figure 9. The measured seasonal temperature probability density with the fitting curve of the prototype bridge.

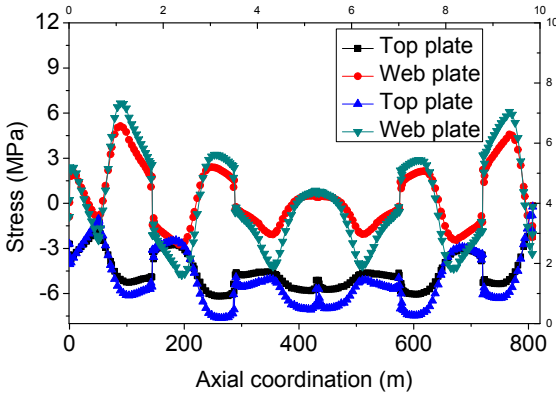

Figure 10. The outline of the temperature stress envelope of the top plate and bottom plate of the bridge.

Combining Equation (5), using the data processed in Section 4.2, we can get the fatigue damage variation law corresponding to the embedded sensor position during the design basis period of 100 years, as seen in **Figures 11 and 12**.

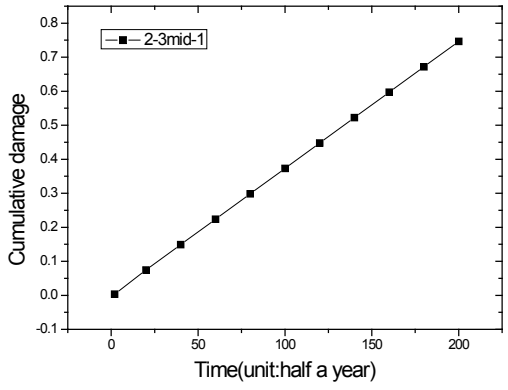

Figure 11. The change of the cumulative damage in 100 years is calculated by the monitoring data of 2-3 mid-1.

At the mid-span top plate, the one-year damage value is 0.0037338 which is obtained by using the monitoring data of the sensor 2-3 mid-1, and the cumulative damage value during the design basis period (100 years) is 0.7468; At the mid-span web plate, the one-year damage value is 0.0002648 which is obtained by using the monitoring data of the sensor 3-4 mid-2, and the cumulative damage value during design basis period (100 years) is 0.053. Based on the data in **Figures 11 and 12**, using Equation (6), we got $L(T_s) > 0$ in the design basis period of the bridge. Then, we can draw a conclusion that the calculated damage variation rules and damage degree are in line with the design requirements of relevant specifications of the concrete bridge structures. At the same time, compared with the bridge web plate, the position of the top plate is more sensitive to fatigue damage, and the main reason may be the large variation range of live load stress at the position of a top plate of the bridge.

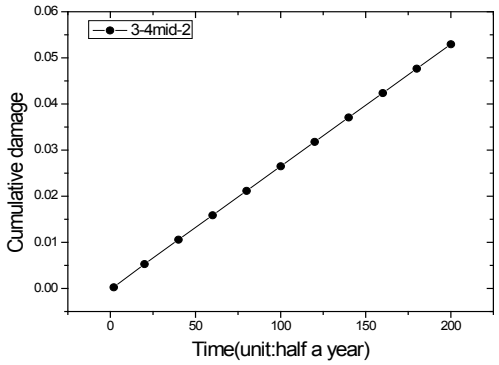

Figure 12. The change of the cumulative damage in 100 years is calculated by the monitoring data of 3-4 mid-2.

5. Conclusions

Adopting a large amount of strain monitoring data collected from the HMS of the bridge, combining fatigue damage theory and Miner rule, in the article, we proposed a method for calculating the fatigue damage of bridge structures, and the main conclusions are:

(1) By using S-N curves of the concrete material used in the bridge and linear accumulation damage with the Miner rule, the formulas of fatigue damage calculation and accumulation are derived.

(2) Based on a large amount of stress data transformed from the strain monitoring data, using the

rain flow counting method, the fatigue stress spectrum of the bridge was obtained, and it is found by calculation that the damage degree is consistent with the design requirements of the specifications, and also found that the position of the top plate is more sensitive to fatigue damage.

(3) The fatigue damage value calculated in this paper may be small, mainly due to the small number of traffic flow statistics and the deterioration of concrete material strength. So, it is necessary to use actual traffic flow survey data and the change law of concrete strength to correct the fatigue damage value during different service periods of the bridge calculated in this paper.

(4) In the next step of work, we should focus on the framework for the integration of fatigue damage analysis and HMS concepts into bridge maintenance management decision making. At the same time, considering the components and system reliability would be helpful for the development of maintenance strategies during the fatigue design basis period.

Conflict of Interest

There is no conflict of interest.

Acknowledgement

The authors are very grateful for the strong help of the collaborators. Without their help, this article could not been finished.

References

[1] Moodi, F., Knapton, J., 2003. Research into a management system for diagnosis, maintenance, and repair of concrete structures. Journal of Construction Engineering and Management. 129(5), 555-561.

[2] Rokugo K , Hatano H , Banthia N., 2008. Report on the Collapse of de la Concorde Overpass in Canada (Japanese) [Report on the collapse of de la concorde overpass in Canada]. Concrete Journal. 46(12), 35-41. DOI: https://doi.org/10.3151/coj1975.46.12_35

[3] Gong, J.X., Wang, H.C, Li, J.B., 2005. He zai dui xiu shi huan jing xia gang jin hun ning tu liang xiu shi de ying xiang (Chinese) [Effect of load on corrosion of reinforced concrete beams in corrosive environment]. Journal of Southeast University (Natural Science Edition). 35(3),421-426.

[4] Song Y.P, Han J.G., 2021. Pi lao he zai zuo yong xia bu tong xing gang liang de po huai guan xi (Chinese) [Failure relationship of different types of steel bars in beams under fatigue load]. Journal of Harbin Institute of Technology. 44(8), 96-100.

[5] Study on Fatigue Behavior of Corroded RC Beam [Internet]. Available from: https://www.researchgate.net/profile/V-Feldgun/publication/283292537_A_new_equation_of_state_for_cementitious_materials_-_a_multiscale_approach/links/565184cc08aefe619b161800/A-new-equation-of-state-for-cementitious-materials-a-multiscale-approach.pdf#page=475

[6] Gao, Z., Liang, R.Y., Patnaik, A.K., 2016. Effects of sustained loading and pre-existing cracks on corrosion behavior of reinforced concrete slabs. Construction and Building Materials. 124, 776-785.

[7] Sun, J., Ding, Z., Huang, Q., 2019. Development of EIFS-based corrosion fatigue life prediction approach for corroded RC beams. Engineering Fracture Mechanics. 209, 1-16.

[8] Guo, Z., Ma, Y., Wang, L., et al., 2020. Crack propagation-based fatigue life prediction of corroded RC beams considering bond degradation. Journal of Bridge Engineering. 25(8), 04020048.

[9] Wen, B., 2021. Gang jing hun ning tu jie gou pi lao tui hua ji li ji xing neng ti shen ji shu (Chinese) [Fatigue degradation mechanism and performance improvement technology of reinforced concrete structures] [Ph.D. thesis]. Nanjing: Southeast University.

[10] Li, Z.X., Chan, T.H., Ko, J.M., 2001. Fatigue analysis and life prediction of bridges with structural health monitoring data—Part I: Meth-

odology and strategy. International Journal of Fatigue. 23(1), 45-53.

[11] Chan, T.H., Li, Z.X., Ko, J.M., 2001. Fatigue analysis and life prediction of bridges with structural health monitoring data—Part II: Application. International Journal of Fatigue. 23(1), 55-64.

[12] Tong, G., Aiqun, L., Jianhui, L., 2008. Fatigue life prediction of welded joints in orthotropic steel decks considering temperature effect and increasing traffic flow. Structural Health Monitoring. 7(3), 189-202.

[13] Kwon, K., Frangopol, D.M., 2010. Bridge fatigue reliability assessment using probability density functions of equivalent stress range based on field monitoring data. International Journal of Fatigue. 32(8), 1221-1232.

[14] Deng, Y., Ding, Y., Li, A., et al., 2011. Fatigue reliability assessment for bridge welded details using long-term monitoring data. Science China Technological Sciences. 54, 3371-3381.

[15] Newhook, J.P., Edalatmanesh, R., 2013. Integrating reliability and structural health monitoring in the fatigue assessment of concrete bridge decks. Structure and Infrastructure Engineering. 9(7), 619-633.

[16] Junges, P., Pinto, R.C.A., Miguel, L.F., 2018. Fatigue life assessment of reinforced concrete bridges from monitoring data. Maintenance, safety, risk, management and life-cycle performance of bridges. CRC Press: Boca Raton. pp. 634-641.

[17] Mankar, A., Bayane, I., Sørensen, J.D., et al., 2019. Probabilistic reliability framework for assessment of concrete fatigue of existing RC bridge deck slabs using data from monitoring. Engineering Structures. 201, 109788.

[18] Miner, M.A., 1945. Cumulative damage in fatigue. Journal of Applied Mechanics. 12(3), 159-164.

[19] Song Y.P, 2004. Gang jin hun ning tu jie gou (Chinese) [Reinforced Concrete Structure]. Beijing: China Machine Press.

[20] GB 50010-2010 (2015) Code for Design of Concrete Structures [Internet]. Available from: https://www.codeofchina.com/standard/GB50010-2010(2015).html

[21] CCCC Highway Planning and Design Institute, 2012. Standard of the Ministry of Communications of P. R.C. specifications for design of highway reinforced concrete and prestressed concrete bridges and culverts (JTG 3362-2018). China Communications Press: Beijing.

[22] Liu, Z.J., Li, Y.H., Tang, L.Q., et al., 2014. Localized reliability analysis on a large-span rigid frame bridge based on monitored strains from the long-term SHM system. Smart Structures & Systems. 14(2), 209-224.

[23] Li, Y., Peng, K., He, J., et al., 2021. Maintenance management research of a large-span continuous rigid frame bridge based on reliability assessment by using strain monitored data. Journal of Architectural Environment & Structural Engineering Research. 4(2), 20-31.

[24] Zhang Y., 2015. Che liang zong cheng xing neng jian ce ji shu (Chinese) [Vehicle assembly performance detection technology]. Beijing: National Defense Industry Press. Available from: https://www.amazon.fr/%E8%BD%A6%E8%BE%86%E6%80%BB%E6%88%90%E6%80%A7%E8%83%BD%E6%A3%80%E6%B5%8B%E6%8A%80%E6%9C%AF-%E5%BC%A0%E9%9B%A8/dp/B01AUNRXP6

[25] About MATLAB [Internet]. Available from: https://ww2.mathworks.cn/products/matlab.html

[26] Li, Y.H., 2021. Ji yu chang qi jian kang jian de hun ning tu lian xu gang gou liang qiao xing neng fen xi yu yan hua gui lv yan jiu (Chinese) [Performance analysis and evolution of continuous rigid frame girder bridges based on long-term health monitoring]. Guangzhou: South China University of Technology. Available from: https://cglhub.com/auto/db/detail.aspx?db=950008&rid=1283605&agfi=0&cls=0&uni=True&cid=0&showgp=True&prec=False&md=152&pd=208&msd=152&psd=208&mdd=152&pdd=208&count=10&reds=submodeling